Available online at www.sciencedirect.com

ScienceDirect

Procedia Structural Integrity 2 (2016) 2674–2681

Structural Integrity Procedia

www.elsevier.com/locate/procedia

21st European Conference on Fracture, ECF21, 20-24 June 2016, Catania, Italy

A non-linear constitutive relation for the analysis of FRCM elements

Bernardi P., Ferretti D., Leurini F.*, Michelini E.

DICATeA, University of Parma, Parco Area delle Scienze 181/A, 43124 Parma, Italy

Abstract

Nowadays, the strengthening of existing buildings represents one of the most innovative fields within current research in civil engineering. Among the developed techniques, a recent solution consists in the use of FRCM composites (Fabric Reinforced Cementitious Matrix), which are obtained by placing a dry grid of fibers inside a cement-based material (mortar). In comparison with traditional systems, the use of FRCM seems to provide some advantages; however, a full understanding of the mechanical properties of each component (mortar and fibers) and of their interaction, as well as their effect on the strengthened structure, still represents an open research topic. This work aims to be a first attempt to numerically simulate the global behavior of FRCM composites through the development of a macroscopic constitutive model subsequently implemented into a Non-Linear Finite Element (NLFE) procedure. The effectiveness of the proposed procedure is verified through comparisons with significant experimental results available in technical literature, relative to FRCM tension ties. The influence exerted by the adoption of different materials (such as Poliparafenilenbenzobisoxazolo (PBO) and carbon) for the internal fiber grid on the global behavior is also analyzed and discussed.

Peer-review under responsibility of the Scientific Committee of ECF21.

Keywords: FRCM; strenghtening; smeared models; Non-Linear Finite Element Analysis; tension ties

1. Introduction

Fabric Reinforced Cementitious Matrix (FRCM) is a new type of strengthening technique for reinforced concrete and masonry structures, which consists of a layer of cementitious matrix that includes in the middle one or more nets

* Corresponding author. Tel.: +39-0521-905709; fax: +39-0521-905924.
E-mail address: filippo.leurini@studenti.unipr.it

Peer review under responsibility of the Scientific Committee of ECF21.
10.1016/j.prostr.2016.06.334

of fibers. It must be placed so that the layer of this matrix is smeared onto the element that has to be strengthened. Since matrix characteristics are similar to those of the support, the adhesion between the reinforcement and the structure that has to be retrofitted is very good. Mortar is indeed a cement-based material, generally enriched with filaments of different materials (like Alkali Resistant (AR) glass) and polymers to improve its workability and mechanical properties. PBO, carbon and glass commonly constitutes the grid of fibers, which is placed into the layer of mortar. This new composite material offers some advantages over more traditional strengthening techniques, such as Fiber Reinforced Polymers (FRP). Firstly, FRCM seems to show a better compatibility with historical buildings and offers a higher fire resistance. Secondly, its performances under freeze-thaw cycles are better and it is characterized by a higher water vapor permeability and a lower toxicity.

For these reasons, several producers and researchers in the recent past have started to show interest in this technique and different types of tests have been proposed in order to study its effectiveness. Among them, one of the most common is the direct tensile test that allows investigating the constitutive law of the material (Mobasher et al. (2006), Contamine et al. (2011), De Santis and De Felice (2015), Carozzi and Poggi (2015)). Other tests, like single or lap shear ones, have been carried out to point out other mechanical properties, like bond between mortar and the fiber grid (D'Antino et al. (2014), Sneed et al. (2014), D'Ambrisi et al. (2012), Carozzi and Poggi (2015)).

This paper is mainly focused on tensile tests, which can show different stress-strain paths or failure modes depending on the adopted test setup. The American Design Code (AC434 (2013)) suggests the use of a "Clevis" grip at the ends of the specimen. In this case, the load is transmitted by tangential stresses on the mortar and no normal pressure is exerted on the sample. Failure occurs due to the slippage of fibers with respect to the matrix and consequently a bilinear average stress strain law is expected. Conversely, according to the clamping method more adopted in Europe (RILEM 232-TDT (2014)), the load is transmitted to the specimen surface through shear and normal stresses. In this way, the fibers are prevented from slipping within the mortar and a trilinear law can be obtained. Therefore, a complete characterization of the composite material is possible, since each component (mortar and fiber net) is lead to failure during the test, differently from the use of Clevis grip device, where only mortar fails.

Aim of this paper is to develop a non-linear constitutive model able to simulate the behavior up to failure of this strengthening system and to take into account the different resistant contributions occurring after crack formation. The proposed approach is subsequently validated through experimental data from literature, relative to significant tensile tests (Carozzi and Poggi (2015)).

2. A non-linear constitutive model for FRCM

A non-linear constitutive model is developed herein. This relation simulates the behavior of FRCM by taking into account the mechanical properties of its components. It is meant to be adopted in conjunction with Finite Element (FE) technique and it is based on a continuum approach, where all the fundamental quantities are smeared within the element.

According to the model, a FRCM element subjected to a general plane stress state is considered (Fig.1). Before cracking, the composite material is assumed as linear elastic and thus the element behavior is determined only on the basis of the elastic modulus and the Poisson's coefficient of the two components (mortar and fiber net).

In the cracked stage, cracks are assumed as fixed and equally spaced, and the post-cracking behavior is assumed to be ruled by several contributions. In more detail, the bridging action of the aggregates and of the dispersed filaments of fibers and polymers is taken into account for mortar, while the fundamental resistant contribution considered for fiber net is tension stiffening. Realistic semi-empirical constitutive laws are included in the model to represent these effects.

The model is organized in a modular framework; therefore, all the mechanical contributions are separately modeled and each part of the algorithm can be modified independently from others. Its basic structure is inspired to an analogous constitutive relation developed for the analysis of reinforced concrete elements (2D-PARC, Cerioni et al. (2008)).

The model is written in a Fortran routine to be implemented as user-defined material (UMAT) into a commercial finite element code (ABAQUS). Given the attained total strains, at each time increment of the analysis the model, through this UMAT, provides to the FE Code the stress field and the global material stiffness matrix for each

integration point of the mesh. All the convergence checks are then performed by the FE code, according to the chosen criteria. In the following, a more detailed description of the model is presented.

2.1. Basic assumptions

A FRCM membrane element with thickness *s* and subjected to a general plane stress state is considered. For this element, depicted in Figure 1, a global system coordinate (*x,y*) is defined, whose directions are assumed to be parallel to element sides, as well as to the two orientations of the reinforcement, consisting of a fiber net. In the cracked stage, characterized by equally spaced cracks at a distance a_m, a local system coordinate (*n,t*) is also adopted, where *n* and *t* axes respectively denote the directions normal and tangential to the crack (Fig.1). The geometric reinforcement ratio, that is the ratio between the area of fibers and the transversal area of mortar, is indicated with ρ_{ri}, where subscript "*i*" (*i*=1,2) denotes the two fiber orders of the net.

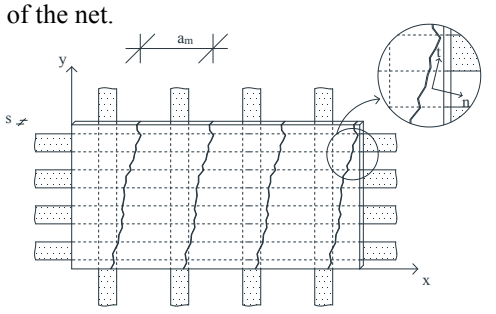

Fig. 1. Sketch of the considered FRCM element, with the indication of the global *(x,y)* and local (*n,t*) coordinate systems.

2.2. Uncracked stage

At this stage, perfect bond between mortar and fiber net reinforcement is assumed. Thus, the corresponding strain vectors $\boldsymbol{\varepsilon}_{\mathbf{m}}$ and $\boldsymbol{\varepsilon}_{\mathbf{r}}$ can be considered coincident with the total strain vector $\boldsymbol{\varepsilon}$, as follows:

$$\boldsymbol{\varepsilon} = \boldsymbol{\varepsilon}_{\mathbf{m}} = \boldsymbol{\varepsilon}_{\mathbf{r}} . \tag{1}$$

Consequently, the total stress $\boldsymbol{\sigma}$ results from the sum of the stress in the mortar, $\boldsymbol{\sigma}_{\mathbf{m}}$, and in the fiber net, $\boldsymbol{\sigma}_{\mathbf{r}}$, and the global uncracked stiffness matrix of the composite can be expressed as the sum of the stiffness matrices relative to each single material. By assuming a linear elastic behavior, the mortar stiffness matrix $\mathbf{D}_{\mathbf{m}}$ is simply function of mortar elastic modulus E_m and Poisson's coefficient ν_m:

$$\mathbf{D}_{\mathbf{m}} = \frac{1}{1-\nu_m^2}\begin{bmatrix} E_m & \nu_m \cdot E_m & 0 \\ \nu_m \cdot E_m & E_m & 0 \\ 0 & 0 & (1-\nu_m^2)\cdot G_m \end{bmatrix}, \tag{2}$$

where $G_m = E_m / 2\cdot(1+\nu_m)$ is the shear modulus of the mortar. Similarly, the fiber net reinforcement stiffness matrix $\mathbf{D}_{\mathbf{r}}$ depends only on fiber elastic modulus E_{ri} and on the reinforcement ratio ρ_{ri}:

$$\mathbf{D}_{\mathbf{r}} = \sum_{i=1}^{2} \mathbf{D}_{\mathbf{ri}} = \sum_{i=1}^{2} \rho_{ri} \begin{bmatrix} E_{ri} & 0 \\ 0 & G_{ri} \end{bmatrix}, \tag{3}$$

$G_{ri} = E_{ri} / 2\cdot(1+\nu_{ri})$ being the shear modulus of the *i*-th fiber order. It can be observed that in the examined case of FRCM tension ties, the only significant fiber direction is that parallel to element longitudinal axis (i.e. *i*=1).

From the compatibility Equation (1) and by imposing the equilibrium condition, the stress state in the elements is defined as following, the global stiffness matrix $\mathbf{D}$ being equal to the sum $\mathbf{D}_{\mathbf{m}}+\mathbf{D}_{\mathbf{r}}$:

$$\boldsymbol{\sigma} = \mathbf{D_m}\boldsymbol{\varepsilon_m} + \mathbf{D_r}\boldsymbol{\varepsilon_r} = \mathbf{D}\boldsymbol{\varepsilon} \,. \tag{4}$$

2.3. Cracked stage

When the maximum principal tensile stress attains mortar tensile strength, the material is assumed as cracked. Crack pattern develops immediately, with a constant spacing a_m. The assumption of perfect bond is no longer valid and according to the model hypotheses, the total strain $\boldsymbol{\varepsilon}$ can now be obtained by summing up the strain of mortar between two adjacent crack $\boldsymbol{\varepsilon_m}$, and that of the composite material in the fracture zone $\boldsymbol{\varepsilon_{cr}}$, this latter being produced by all the mechanisms developing after the crack formation. Therefore, the total strain can be written as:

$$\boldsymbol{\varepsilon} = \boldsymbol{\varepsilon_m} + \boldsymbol{\varepsilon_{cr}} \,, \tag{5}$$

For the equilibrium condition in uncracked FRCM (Eq. 4) and for that in the crack, $\boldsymbol{\varepsilon_m}$ and $\boldsymbol{\varepsilon_{cr}}$ can be respectively obtained through the following relations:

$$\boldsymbol{\varepsilon_m} = \mathbf{D_m}^{-1}\left(\boldsymbol{\sigma} - \mathbf{D_r}\,\boldsymbol{\varepsilon_r}\right), \tag{6}$$

$$\boldsymbol{\varepsilon_{cr}} = \mathbf{D_{cr}}^{-1}\boldsymbol{\sigma} = \left(\mathbf{D_{m,cr}} + \mathbf{D_{r,cr}}\right)^{-1}\boldsymbol{\sigma} \,, \tag{7}$$

$\mathbf{D_{cr}}$ taking into account all the resistant contributions in the crack, referred both to mortar ($\mathbf{D_{m,cr}}$) and to fiber net reinforcement ($\mathbf{D_{r,cr}}$).

2.3.1. Mortar contribution in the crack

The mortar adopted in the composite material generally includes the addition of fibers and polymers, which, besides improving the mechanical characteristics of the compound, have the aim of stabilizing crack development by reducing crack openings. After crack formation, the presence of AR glass filaments and polymers dispersed in the mortar provides a stiffening contribution, due to the bridging effect across the crack. This action must be properly modeled and included in $\mathbf{D_{m,cr}}$ matrix. To this aim, reference is made herein to a microscopic model originally developed by Li et al. (1993) for fiber-reinforced concrete. According to this model, bridging effect in fiber reinforced cementitious composites can be mainly attributed to aggregates and fibers in the matrix. These latter can exert two main actions: the first one, so-called "fiber bridging", depends on the opposition that fibers develop against debonding (fiber pull-out), the second one, referred to as "fiber prestressing", is instead related to fiber prestress before cracking (Li (1992)).

Once again, only the basic structure of this model is followed in this work, but aggregate bridging provided by plain mortar is here considered instead of that of concrete. Those contributions are written as a function of the crack opening and depend on the mechanical characteristics of mortar, on fiber dimensions, as well as on fiber volume fraction.

Aggregate bridging action is obtained from the tension-softening curve of plain mortar. This latter is calculated according to the model of Ishiguro (2007), which first evaluates a limit crack opening w_c as function of mortar fracture energy G_f (this last is dependent from mortar compressive strength f_c) and tensile strength f_{ct}, through the expressions:

$$w_c = 4.7\frac{G_f}{f_{ct}} \text{, where: } G_f = 0.0251 \cdot f_c^{\,0.105} \,. \tag{8}$$

Subsequently, the tension softening σ_{ct} - w curve, modelled with a hyperbolic function, can be obtained as:

$$\sigma_{ct} = f_{ct}\,\frac{c_1 - c_1 \cdot w/w_c}{c_1 + w/w_c} \,, \tag{9}$$

where w is the current crack width and c_1 a constant factor equal to 0.168. The effectiveness of these correlations is confirmed by the good agreement with experimental data from extensive testing on different types of mortar (Ishiguro (2007)).

By following the general formulation developed in Cerioni et al. (2008), the bridging coefficient c_b to be inserted into the cracked mortar stiffness matrix $\mathbf{D_{m,cr}}$ can be defined as:

$$c_b = \frac{\sigma_{ct} \cdot a_m}{w}. \tag{10}$$

The basic role of AR glass filaments and polymers in the mortar is to increase the bridging action. This is taken into account through fiber bridging stress σ_f and fiber prestress σ_{ps}, which are evaluated according to Li (1992) as function of fiber geometric and mechanical properties. Once again, the corresponding coefficient c_f appearing in cracked mortar stiffness matrix can be obtained through the following expression (Cerioni et al. (2008)):

$$c_f = \frac{\left(\sigma_f + \sigma_{ps}\right) \cdot a_m}{w}. \tag{11}$$

It must be observed that, differently from plain concrete, aggregate interlock is not so relevant in plain mortar for the absence of gravel in the admixture.

Finally, the mortar matrix in the crack, accounting for aggregate bridging and fiber contributions assumes the form:

$$\mathbf{D_{m,cr}}^{(n,t)} = \begin{bmatrix} c_b + c_f & 0 \\ 0 & c_f \end{bmatrix}. \tag{12}$$

This matrix is first written in the local coordinate system of the crack (n,t), and then transposed into the global (x,y) one (see Fig. 1 for nomenclature) through a proper transformation matrix, which is function of the angle between the global x-axis and the local n-axis.

2.3.2. Fiber net reinforcement contribution in the crack

As already mentioned, in the FRCM system the reinforcement is constituted by one or more fiber nets placed within a layer of mortar. Since fibers are made of dry fabric, the mortar does not fully impregnate them and so two different types of slippage could typically occur, either between matrix and fibers in direct contact, or within the yarns (telescopic failure, Banholzer (2004)). For sake of simplicity, this last type of failure is not covered from the present model, which only simulates the loss of bond between the fabric and the mortar.

In order to evaluate the stiffening contribution exerted by the fiber net on adjacent mortar, it is necessary to consider the interaction between these two materials. To this aim, many experimental programs have been studied, providing several bond-slip relations for different types of fiber net and surrounding mortar (Sneed et al. (2014), D'Ambrisi et al. (2012), D'Ambrisi et al. (2013)).

In the proposed model, the problem is solved by following the approach of Cerioni et al. (2008), and by introducing a "tension stiffening coefficient", which takes into account the fiber net reinforcement stiffening contribution after cracking. This coefficient, named g_i, is given by the ratio between the axial fiber net reinforcement strain in the crack and the crack strain itself. The strain distribution along fibers is evaluated by numerically solving the classic second order bond-slip differential equation, through the Finite Difference method. To this aim, a proper bond-slip relation for FRCM is assumed. In this work, Model Code 2010 (2012) bond-slip law is adopted, by properly calibrating its parameters on the basis of the experimental laws proposed by D'Antino et al. (2014) and D'Ambrisi et al. (2013), for PBO fibers and for carbon fibers, respectively.

The tension stiffening coefficient modifies the fiber elastic modulus E_{ri} and so, by neglecting the fiber shear modulus, the cracked fiber net reinforcement stiffness matrix $\mathbf{D_{ri,cr}}$ for the i-th fiber direction can be obtained as:

$$\mathbf{D}_{\mathbf{ri,cr}} = \rho_{ri}\begin{bmatrix} E_{ri}\cdot g_i & 0 \\ 0 & 0 \end{bmatrix}. \tag{13}$$

2.3.3. Material between adjacent cracks

The behavior of the composite material between adjacent cracks is assumed the same as in the uncracked stage. Consequently, the same stiffness matrices reported in Equations (2) and (3) are adopted for mortar and fiber net reinforcement. Anyway, the strain distribution along the fiber net is not-uniform due to tension stiffening effect. Because of the smeared formulation of the model, for sake of simplicity the strain of fibers net reinforcement in uncracked material between cracks $\boldsymbol{\varepsilon_r}$ is assumed equal to the global average strain $\boldsymbol{\varepsilon}$ of the element. Consequently, this value is substituted into Equation 4 in order to evaluate the mortar strain $\boldsymbol{\varepsilon_m}$. As already mentioned, the tension stiffening effect is explicitly taken into account in the cracked fiber net reinforcement matrix (Eq. 13).

3. Comparisons with experimental testing by Carozzi and Poggi (2015)

The effectiveness of the above described procedure is verified through comparisons with detailed test data. Among others, an experimental program carried out by Carozzi and Poggi (2015) on FRCM tension ties is considered. The objective of these tests was the mechanical characterization of FRCM material; in particular, trilinear laws describing their behavior in tension were provided.

The herein analyzed tensile tests concerned rectangular specimens, whose dimensions (400 x 40 x 10 mm) are reported in Figure 2 (right side). FRCM material was composed by a cementitious matrix including a low volumetric percentage of polymers and AR glass filaments. PBO, carbon or glass fiber nets were adopted as reinforcement. This paper is focused on the simulation of ties with PBO or carbon nets. The main experimental mechanical properties of mortar and fibers are synthetically recalled in Table 1.

As regards test set up, the ends of each specimen were fixed into the grips of a mechanical testing machine and then the sample was subjected to tension by applying an increasing displacement. The adopted clamping system allowed for torsional rotation in the lower grip, being configured differently from AC434 (2013) prescriptions. Consequently, since the two specimen ends could be subjected to high compressive stresses, fiber reinforced plates (60 x 40 x 2 mm, Fig.2) were glued to the element. During the test, an extensometer with a gauge length of 100 mm was placed in the central area of the specimen to measure displacements. Crack path development was recorded at different loading stages by adopting digital image correlation.

The chosen system allowed determining the ultimate tensile strain and strength, as well as the modulus of elasticity of mortar both in the uncracked and cracked stage. The typical trilinear behavior was observed experimentally, characterized by a first phase, where the specimen is uncracked and its behavior is more or less that of the mortar, a second "transition" phase, where the cracks develop, and finally a last stage with completely cracked mortar. In this last stage, only the fiber net contributes in carrying the external load.

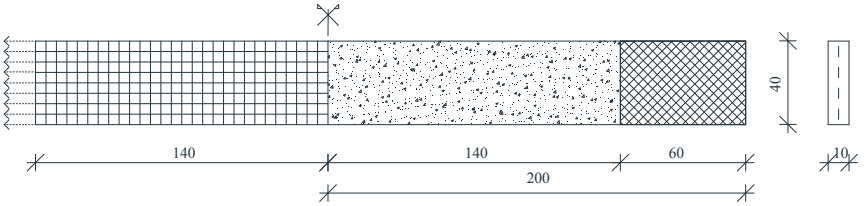

Fig. 2. On the right: sketch of the specimen with metal plate at one end and cross-section with indication of fiber net in the middle (dotted line). On the left: FE mesh (not including the clamped end) and applied displacement (all dimensions in mm).

3.1 NLFE analyses

NLFE analyses are performed to simulate the above described tensile tests. The proposed constitutive model for FRCM is adopted to the scope, and implemented into a commercial FE code (ABAQUS) to predict the tensile behavior of the considered specimens. A mesh of 8-node membrane elements with reduced integration (M3D8R) and average

FE size of 5 mm is adopted. By taking advantage of the symmetry of the problem only one half of the specimen is modelled. Consequently, in the middle section proper symmetry constraints are applied, while on the free edge an increasing displacement is applied (Fig. 2, left side).

As regards material mechanical properties adopted in numerical simulations, reference is basically made to the experimental ones (Carozzi and Poggi (2015)). For fibers, only two parameters (i.e. the elastic modulus and the average failure stress or strain) are needed for their complete characterization, since the behavior can be assumed as linear elastic until failure (Table 1). On the contrary, major uncertainties lies on mortar mechanical properties. From experimentation, only the mortar tensile strength obtained from Brazilian test ($f_{ct,\,split}$) is provided. Since the proposed constitutive model requires direct tensile strength f_{ct} (to be inserted into Eq. 9), the latter is deduced from the experimental value of $f_{ct,\,split}$, by adopting a correlation factor similar to the one used for concrete, which can range between 0.8 and 0.9. So, the correlation $f_{ct} = 0.85\, f_{ct,\,split}$ is here tentatively adopted. Furthermore, in order to take into account the strength variation along the specimen, the lower bound of mortar tensile strength is assumed in the analysis, referred to 5% fractile, i.e. $f_{ctk,0.05}=0.7 \cdot f_{ctm}$. As it will shown below, this assumption allows achieving a good fitting with experimental evidences. The resultant values for mortar in specimens with PBO or carbon fiber reinforcement are reported in Table 1. The same Table also summarizes the mortar elastic modulus E_m and the mortar compressive strength f_c, which are deduced by other experimental tests concerning the same material (Alecci et al. 2016).

Table 1. Materials mechanical properties (Carozzi and Poggi (2015), Alecci et al. (2016)).

Material	E [GPa]	ε_u [-]	$f_{ctk,0.05}$ [MPa]	f_c [MPa]
PBO fibers	215.9	0.0155		
Carbon fibers	203.0	0.0094		
Mortar for PBO specimen	2.87		3.65	20.2
Mortar for Carbon specimen	2.87		2.02	20.2

3.2 Comparisons between numerical and experimental results

Comparisons are provided in terms of stress-strain behavior for each type of fiber grid material (Fig. 3). In more detail, three experimental curves are plotted in Figure 3, which refer to the maximum and minimum envelopes of all the experimental curves and to the average trend provided by the Authors (Carozzi and Poggi (2015)). It must be underlined that stresses are computed by dividing the forces applied to the specimen by the area of fibers. This is necessary because the area of mortar is not always perfectly the same, given the small size of the specimens.
Numerical results are obtained through the above described non-linear procedure. As can be observed from the reported graphs, a good agreement between numerical and experimental responses is achieved. The major approximation can be observed immediately after the formation of the first crack; this is related to the fact that in this stage the behavior of tension ties is mainly ruled by the bridging of the aggregates and so the numerical response is governed by the tension softening law adopted for mortar.

The lack of a well-defined tri-linear behavior in numerical curves can be explained by the fact that the adopted constitutive model for FRCM is smeared, and it is based on the assumption that after the reaching of mortar tensile strength the crack pattern develops immediately and it is not gradual.

For PBO-FRCM specimens (Fig. 3a), two simulations are made by varying fiber elastic modulus, which essentially affects the third stage behavior. It should be noticed that this value is affected by a certain dispersion, as highlighted by the high covariance of the data provided by the Authors (Carozzi and Poggi (2015)). By adopting the experimental (Carozzi and Poggi (2015)) value of fiber elastic modulus (equal to 215.9 GPa), in the last third phase the numerical curve shows a higher slope with respect to the experimental one. So, the same analysis is repeated by considering a lower value of fiber elastic modulus, which is deduced from the effective slope of the experimental average stress-strain curve, resulting in the value of 181.7 GPa. For carbon-FRCM specimens (Fig. 3b), the experimental value of fiber elastic modulus declared by Authors (Carozzi and Poggi (2015)) is used. In this case, the numerical analysis provides a response that is quite close to the higher experimental envelope.

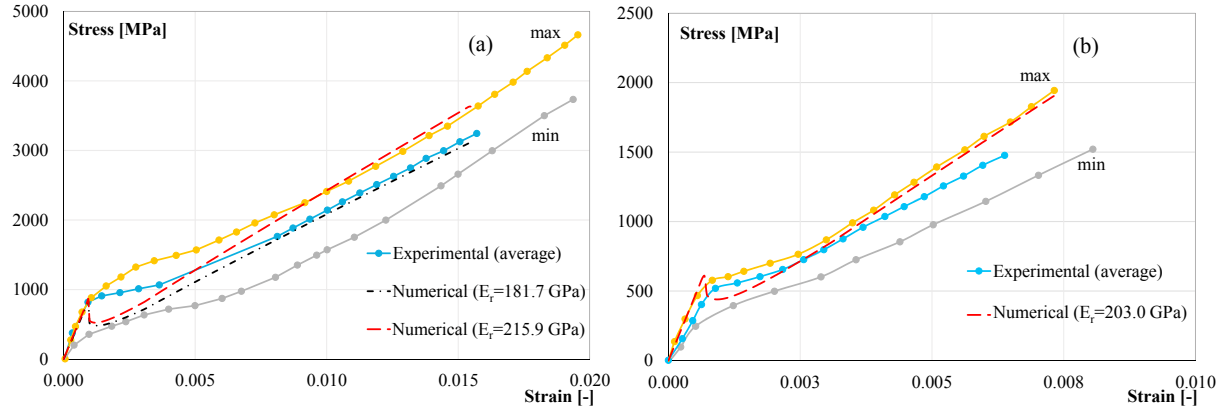

Fig. 3. Comparisons between numerical and experimental (Carozzi and Poggi (2015)) results: (a) PBO-FRCM (b) Carbon-FRCM specimens.

4. Conclusions

In this paper, a non-linear constitutive model for the analysis of the behavior of FRCM elements is presented. The procedure is verified through comparisons with experimental data on FRCM rods, providing satisfactory results in terms of global behavior. A fundamental feature in the modelling concerns the need of a proper knowledge of mortar mechanical properties and behaviour, particularly after cracking, which could improve numerical results.

Possible future developments will concern the modelling of RC beams strengthened with this new composite material.

References

AC434, 2013. Masonry and Concrete Strengthening Using Fiber-reinforced Cementitious Matrix (FRCM) Composite Systems. ICC-Evaluation Service. Whittier (CA).

Alecci, V., de Stefano, M, Luciano, R., Rovero, L., Stipo, G., 2016. Experimental Investigation on Bond Behavior of Cement-Matrix–Based Composites for Strengthening of Masonry Structures. Journal of Composites for Construction 20.

Banholzer, B., 2004. Bond behavior of a Multi-Filament yarn embedded in a cementitious Matrix. Ph.D. thesis, RWTH Aachen University.

Carozzi, F.G., Poggi, C., 2015. Mechanical properties and debonding strength of Fabric Reinforced Cementitious Matrix (FRCM) systems for masonry strengthening. Composites Part B: Engineering 70, 215-230.

CEB-FIP Bulletin No.65, 2012. Model Code 2010. Final draft – vol. 1. Lausanne: International Federation for Structural Concrete.

Cerioni, R., Iori, I., Michelini, E., Bernardi, P., 2008. Multi-directional modeling of crack pattern in 2D R/C members. Engineering Fracture Mechanics 75, 615-628.

Contamine, R., Si Larbi, A., Hamelin, P., 2011. Contribution to direct tensile testing of textile reinforced concrete (TRC) composites. Materials Science and Engineering: A 528, 8589-8598.

D'Ambrisi, A., Feo, L., Focacci, F., 2012. Bond-slip relations for PBO-FRCM materials externally bonded to concrete. Composites Part B: Engineering 43, 2938-2949.

D'Ambrisi, A., Feo, L., Focacci, F., 2013. Experimental and analytical investigation on bond between Carbon-FRCM materials and masonry. Composites Part B: Engineering 46, 15–20.

D'Antino, T., Carloni, C., Sneed, L.H., Pellegrino, C., 2014. Matrix-fiber bond behaviour in PBO FRCM composites: A fracture mechanics approach. Engineering Fracture Mechanics 117, 94-111.

De Santis, S., de Felice, G., 2015. Tensile behaviour of mortar-based composites for externally bonded reinforcement systems. Composites Part B: Engineering 68, 401-413.

Ishiguro, S., 2007. Experiments and analyses of fracture properties of grouting mortars, 6th International Conference on Fracture Mechanics of Concrete and Concrete Structures – FraMCoS, Catania, Italy.

Li, V.C., 1992. Postcrack scaling relations for fiber reinforced cementitious composites. Journal of Materials in Civil Engineering, 4, 41–57.

Li, V.C., Stang, H., Krenchel, H., 1993. Micromechanics of crack bridging in fibre-reinforced concrete. Materials and Structures 26, 486–494.

Mobasher, B., Pahilajani, J., Peled, A., 2006. Analytical simulation of tensile response of fabric reinforced cement based composites. Cement and Concrete Composites 28, 77-89.

RILEM Technical Committee 232-TDT, 2014. Test methods and design of textile reinforced concrete.

Sneed, L.H., D'Antino, T., Carloni, C., 2014. Investigation of Bond Behavior of Polyparaphenylene Benzobisoxazole Fiber-Reinforced Cementitious Matrix-Concrete Interface. ACI Materials Journal 111, 1–12.